

Supporting Information for:

**Just Add Water: Hydratable, Morphologically Diverse Nanocarrier Powders for Targeted Delivery**

**Authors:**

Sharan Bobbala<sup>1,†</sup>, Michael P. Vincent<sup>1,†</sup>, and Evan A. Scott<sup>1,2,3,4,\*</sup>

**Affiliations:**

<sup>1</sup>Department of Biomedical Engineering, Northwestern University, Evanston, Illinois, USA

<sup>2</sup>Chemistry of Life Processes Institute, Northwestern University, Evanston, Illinois, USA

<sup>3</sup>Simpson Querrey Institute, Northwestern University, Chicago, Illinois, USA

<sup>4</sup>Robert H. Lurie Comprehensive Cancer Center, Northwestern University, Chicago, Illinois, USA

<sup>†</sup>These authors are co-first authors and contributed equally to this work

\*To whom correspondence should be addressed:

Evan Scott, PhD

Assistant Professor of Biomedical Engineering

Northwestern University

2145 Sheridan Road

Evanston, IL 60208

evan.scott@northwestern.edu

## Methods

**Chemicals.** Unless stated otherwise, all chemical materials and reagents were purchased from MilliporeSigma (St. Louis, MO).

**PEG-*b*-PPS synthesis.** PEG-*b*-PPS polymer was synthesized using established procedures described extensively elsewhere<sup>1-5</sup>. Briefly, sodium methoxide was used to deprotect PEG thioacetate. This deprotected PEG thioacetate was then used to initiate the polymerization of propylene sulfide through an anionic ring-opening polymerization reaction. PEG<sub>750</sub> was used as the hydrophilic block of polymersome polymer, whereas PEG<sub>2k</sub> was used as the hydrophilic block for micelle and filomicelle polymers. To promote the self-assembly into micelle, filomicelle, or polymersome morphologies, polymers were synthesized with a specific hydrophilic weight fraction ( $f_{\text{PEG}}$ ), as determined by the relative lengths of PEG starting material and the polymerized PPS chain. A summary of each polymer type used in this study is presented in **Table S1**.

**Peptide synthesis.** Fmoc-N-amido-dPEG<sub>6</sub>-acid was purchased from Quanta Biodesign for use as a PEG spacer. A peptide construct of the form palmitoleic acid-PEG<sub>6</sub>-WHWLPNLRHYAS was synthesized by solid phase peptide synthesis, as described previously<sup>6,7</sup>. The lipid anchored peptide product was >95% pure, as assessed by LC-MS. A cyclic RGD peptide was synthesized as [palmitoleic acid]-[6 unit PEG spacer]-cyclo(RGDFK) using solid phase peptide synthesis using previously described procedures<sup>8</sup>. The lysine residue was used as the attachment point to the PEG spacer.

**Preparation of synthetic polymer-carbohydrate powders.** Powders capable of promoting stable nanocarrier self-assembly upon hydration were prepared using a slurry method. Firstly, PEG-*b*-PPS polymer (10 mg) was dissolved in a volatile organic solvent, dichloromethane (DCM). Carbohydrate (30 mg; mannitol, trehalose, or glucose) was weighed separately and transferred into a 2 ml glass vial with an inner diameter of 12 mm. The organic phase containing the polymer was subsequently added to the carbohydrate powder and mixed using a pipette to form a slurry. Where specified for hydrophobic loading and targeting peptide-display studies, hydrophobic drug cargo or targeting peptide was dissolved in an organic solvent and was subsequently added to this mixture prior to solvent removal. The solvent was evaporated in a vacuum desiccator overnight. Powders containing different carbohydrates (lactose, trehalose, glucose) were also prepared in a similar way as described above using DCM as the organic solvent. Where specified, different volatile organic solvents (acetone, tetrahydrofuran and chloroform) were also utilized to form the powder formulations using mannitol as the carbohydrate.

**Preparation of commercially available polymer amphiphile powders.** PEG-*b*-polystyrene and PEG-*b*-poly(e-caprolactone) were obtained from Polymer Source, Inc. 10 mg of PEG-*b*-polystyrene or PEG-*b*-poly(e-caprolactone) were weighed separately in a vial and dissolved in DCM. The polymer solution was then added to the 2 ml vial containing 30 mg of Mannitol and mixed using a pipette to form a slurry. The organic solvent was subsequently removed overnight in the vacuum desiccator. For loading studies, the hydrophobic cargo was mixed in the polymer solution before adding to the carbohydrate.

**Powder X-ray diffraction (PXRD).** PXRD data were collected at room temperature on an STOE-STADI-P powder diffractometer equipped with an asymmetric curved Germanium monochromator (CuK $\alpha$ 1 radiation,  $\lambda = 1.54056 \text{ \AA}$ ) and one-dimensional silicon strip detector (MYTHEN2 1K from DECTRIS). The line focused Cu X-ray tube was operated at 40 kV and 40 mA. The powder was packed in 3 mm metallic mask and sandwiched between two polyimide layers of tape. Intensity data from 2 to 78 degrees two theta were collected over a period of 30 mins. Instrument was calibrated against a NIST Silicon standard (640d) prior the measurement.

**Preparation of hydrated nanocarriers.** Powders of polymer-carbohydrate mixtures were hydrated with 0.5-1.0 mL of water or PBS (as specified). Samples were briefly vortexed (<1 min) prior to characterization and/or usage in studies. For PEG-*b*-poly(e-caprolactone) powders, after hydration with aqueous media, samples were placed in 60 °C water bath for 30 min for the formation of monodispersed nanocarriers. For loading of hydrophilic molecules into nanocarriers, hydrophilic molecules were dissolved in water or PBS prior to hydration.

**Transmission electron microscopy (TEM) of negatively stained nanostructures.** Nanocarrier samples were negative stained with uranyl formate. Briefly, a 1.0% uranyl formate (UF) negative stain was prepared in ultrapure water, and was adjusted to pH 4.5 via the addition of 10 N KOH (2  $\mu$ l of 10 N KOH/1 mL of UF). The prepared uranyl formate stain was filtered using a 0.45  $\mu$ m nylon filter prior to use. Carbon-coated copper grids (400-mesh) were glow discharged (25 W, 10 s) and 3  $\mu$ l of the nanoparticle sample was applied. Samples were blotted with Whatman filter paper, then were passed through two 30  $\mu$ l volumes of water, followed by two 30  $\mu$ l volumes of 1.0% UF. This procedure leaves ~0.5  $\mu$ l stain on the grid, with an activity of  $2.55 \times 10^{-5} \mu\text{Ci}/\text{grid}$ . Transmission electron microscopy was performed using a JOEL 1400 Transmission Electron Microscope operating at 120 kV. Images were acquired at 30,000X unless otherwise indicated.

**Cryogenic transmission electron microscopy (Cryo-TEM).** Lacey carbon Cu grids (200 mesh) were glow discharged using a Pelco easiGlow glow discharger (Ted Pella). The glow discharging procedure used an atmosphere plasma generated at 15 mA for 15 s with a 0.24 mbar pressure. A 4  $\mu$ l volume was applied to the grid, and was blotted for 5 s with a blot offset of +0.5 mm. Immediately after blotting, the grid was plunged into liquid ethane within a FEI Vitrobot Mark III plunge freezing instrument (Thermo Fisher Scientific). Grids were transferred to liquid nitrogen for storage. A Gatan Cryo Transfer Holder model 626.6 (Gatan) was used to keep plunge-frozen grids vitreous at -180 °C, while viewing on a JOEL JEM1230 LaB6 emission TEM (JOEL USA) at 100 keV. Micrographs were acquired using a Gatan Orius SC1000 CCD camera Model 831 (Gatan).

**Small-angle x-ray scattering (SAXS).** The morphology of hydrated polymersomes was characterized by SAXS performed using synchrotron radiation at the DuPont-Northwestern-Dow Collaborative Access Team (DND-CAT) beamline at the Advanced Photon Source (APS) maintain at Argonne National Laboratory (Argonne, IL, USA). A sample-to-detector distance of approximately 7.5 m was used together with 10 keV ( $\lambda = 1.24 \text{ \AA}$ ) collimated x-rays and a 3 s exposure time. Silver behenate diffraction patterns were used to calibrate the  $q$ -range. Data was analyzed in the  $q$ -range of 0.001 – 0.5  $\text{\AA}^{-1}$ . PRIMUS 2.8.3. was used for data reduction, and SasView 5.0 was used for model fitting. A spherical vesicle model was fit to the data using a chi square ( $\chi^2$ ) minimization procedure, and modeling was performed following established procedures<sup>4</sup>.

**Quantification of peptide loading efficiency.** A mass of peptide construct corresponding to a 5% molar ratio (peptide:polymer) was used to prepare powders consisting of polymer, carbohydrate, and lipid-anchored peptide ligand. Tryptophan fluorescence was used to measure the amount of peptide embedded in nanocarriers after purification using an LH-20 column. Tryptophan fluorescence was measured using a Shimadzu RF-6000 Fluorescence Spectrofluorometer ( $\lambda_{\text{Ex}} = 270 \text{ nm}$ ,  $\lambda_{\text{Em}} = 350 \text{ nm}$ ). Samples were prepared in a quartz cuvette (1 mm path length; Hellma USA, Inc.). Peptide measurements were calibrated against a peptide concentration series (0, 0.06125, 0.125, 0.25, 0.5, and 1.0 mg/mL). Simple linear regression models were calculated in GraphPad Prism software (version 8.4.2).

**Quantification of hydrophobic small molecule encapsulation.** Dil ( $\lambda_{\text{Ex}} = 549 \text{ nm}$ ;  $\lambda_{\text{Em}} = 565 \text{ nm}$ ) fluorescence was measured using a Shimadzu RF-6000 spectrofluorophotometer (Shimadzu). Curcumin loading was determined by measuring the absorbance of 450 nm light using a BioTek Synergy 2 plate reader (BioTek Instruments). Encapsulation efficiency was determined by comparing the fluorescence or absorbance before and after purification with an LH-20 column.

**Hydrophilic biologic encapsulation and loading efficiency characterization.** Hydrophilic encapsulation studies were performed using two hydrophilic cargoes: alkaline phosphatase (AP; Sigma Aldrich) and 70 kDa dextran-tetramethylrhodamine (Dex-TMR; Life Technologies). Briefly, 5 mg of AP and 100  $\mu\text{g}$  of Dex-TMR were dissolved in 1 mL of PBS and this solution was used to hydrate powder consisting of PEG-*b*-PPS PS polymer and mannitol carbohydrate prepared at a 1:3 ratio. The resulting nanocarriers were purified by size exclusion chromatography using a Sepharose 6B column. Dex-TMR ( $\lambda_{\text{Ex}} = 555 \text{ nm}$ ;  $\lambda_{\text{Em}} = 580 \text{ nm}$ ) loading efficiency was measured using a Shimadzu RF-6000 spectrofluorophotometer (Shimadzu). The protein concentration in alkaline phosphatase-loaded PS was determined using the Pierce A660 assay after disrupting the AP-encapsulating PS nanocarriers using 1% Triton-X. The Pierce A660 assay was calibrated against an AP concentration series (0, 0.3, 0.6125, 1.25, 2.5, 5.0 mg/mL AP) (**Fig. S10**). Absorbance was measured using a BioTek Synergy 2 plate reader (BioTek Instruments). Encapsulation efficiency was determined by comparing the fluorescence or absorbance before and after purification by SEC.

**Characterization of enzyme bioactivity.** After hydrating polymersome-forming powders with aqueous media containing AP enzyme (5 mg/mL; Sigma), a fraction of the formulation was purified by SEC as described elsewhere in this methods section. Encapsulated AP enzyme was released by treating nanoparticle suspensions with 1% Triton-X. Samples were incubated with 5-bromo-4-chloro-3-indolyl phosphate (BCIP)/nitro blue tetrazolium (NBT) substrate (Sigma-Aldrich), and enzyme activity was monitored over a 75-minute time interval by measuring the absorbance of 630 nm light using a BioTek Synergy 2 plate reader (BioTek Instruments).

**Macrophage cell culture.** RAW 264.7 macrophages were purchased from ATCC and were cultured in T75 polystyrene tissue culture flasks (BD Biosciences) in Dulbecco's Modified Eagle Medium supplemented with 10% fetal bovine serum (FBS) (Gibco) and 1% penicillin/streptomycin antibiotics (Life Technologies). Cells were passaged by mechanical scraping after reaching 70-80% confluency.

**Primary cell culture.** Human umbilical vein endothelial cells (HUVECs) were purchased from Lonza, Ltd. The HUVECs were cultured in endothelial cell growth basal medium-2 (EBM-2; Lonza) that was supplemented with an EGM-2 BulletKit (Lonza) and FBS (Gibco). All cells were cultured at 37 °C, 5% CO<sub>2</sub> in T25 or T75 flasks. Media was replaced every two days. Cells were passaged by trypsinization.

**MTT assay.** The MTT (3-(4,5-dimethylthiazolyl-2)-2,5-diphenyltetrazolium bromide) assay<sup>9</sup> was performed on cells (n=5/condition) treated with nanocarriers (0.02, 0.2, or 2.0 mg/mL polymer concentration), mannitol (3 mg/mL; Sigma), or Carboplatin (1 mg/mL; Sigma) for 24 h at 37 °C, 5.0% CO<sub>2</sub>. Cells were treated with 0.5 mg/mL thiazolyl blue tetrazolium bromide (MTT) (Sigma) and viability was assessed after 5 h. The absorbance of 570 nm light was measured using a BioTek Synergy 2 plate reader (BioTek Instruments). The percentage of viable cells was calculated by dividing the absorbance of the experimental group by that of the mean fluorescence of PBS-treated cells.

**Flow cytometric analysis of nanocarrier uptake and cytotoxicity.** For each specified cell line, a total of 100,000 cells were seeded per well in 24-well polystyrene plates (Falcon). Cells were allowed to adhere overnight at 37 °C, 4.0% CO<sub>2</sub>. For uptake studies involving endocytosis inhibitor pre-treatments, cells were incubated with either PBS (i.e. no inhibitor), cytochalasin D (CytD, 50  $\mu\text{M}$ ) phagocytosis inhibitor, or chlorpromazine (CPZ, 50  $\mu\text{M}$ ) clathrin-mediated endocytosis inhibitor prior to administering nanocarriers. Inhibitor concentrations were chosen based on published reports<sup>10,11</sup>. Cells were treated with nanocarriers at the specified polymer concentration for 2 h. All cellular incubations were performed at 37 °C, 5.0% CO<sub>2</sub>. After the nanocarrier treatment period, cells were harvested by either mechanical scraping (macrophages) or trypsinization (HUVECs). Cells were stained with fixable Zombie Aqua viability dye (Biolegend) for 20 min at 4 °C to assess cytotoxicity via flow cytometry. A BD LSRFortessa 6-Laser Flow Cytometer was used to perform flow cytometry. A total of 10,000 single cell events were recorded per sample and the resulting data

were analyzed using the Cytobank analysis suite<sup>12</sup>. The median fluorescence intensity (MFI) was normalized by subtracting the average MFI from untreated cells and was used to quantify the cellular uptake of nanocarriers.

**Statistical analysis.** Statistical analyses were performed using GraphPad Prism software (version 9.0.0).

## Supplementary Tables.

Table S1. PEG-*b*-PPS polymers used in this study.

Morphology	Polymer
Micelle (MC) polymer	PEG <sub>45</sub> - <i>b</i> -PPS <sub>23</sub>
Filomicelle (FM) polymer	PEG <sub>45</sub> - <i>b</i> -PPS <sub>44</sub>
Polymersome (PS) polymer	PEG <sub>17</sub> - <i>b</i> -PPS <sub>35</sub>

Table S2. Hydrated nanocarriers prepared from stored powders.

Nanocarrier	Storage duration	Avg. Diameter (nm) <sup>†</sup>	PDI <sup>†</sup>
MC	1 month	29.4	0.08
MC	6 months	26.3	0.12
PS	1 month	96.1	0.11
PS	6 months	64.8	0.18

<sup>†</sup>Number-average diameter and polydispersity index (PDI) determined by dynamic light scattering (DLS).

Table S3. Storage stability of hydrated polymersome suspensions.

Nanocarrier	Storage duration	Avg. Diameter (nm) <sup>†</sup>	PDI <sup>†</sup>
PS	Before storage	77.5	0.15
PS	8 months	68.9	0.14

<sup>†</sup>Number-average diameter and polydispersity index (PDI) determined by dynamic light scattering (DLS).

Table S4. Hydrated nanocarriers from mannitol + polymer powders prepared using alternative organic solvents.

Nanocarrier	Solvent	Avg. Diameter (nm) <sup>†</sup>	PDI <sup>†</sup>
PS	Acetone	64.6	0.30
PS	Chloroform	80.5	0.17
PS	THF	85.7	0.18

<sup>†</sup>Number-average diameter and polydispersity index (PDI) determined by dynamic light scattering (DLS).

Table S5. Hydrated nanocarriers from powders prepared in THF with alternative carbohydrates.

Nanocarrier	Carbohydrate	Avg. Diameter (nm) <sup>†</sup>	PDI <sup>†</sup>
PS	Glucose	69.5	0.19
PS	Lactose	54.1	0.21
PS	Trehalose	78.1	0.14

<sup>†</sup>Number-average diameter and polydispersity index (PDI) determined by dynamic light scattering (DLS).

Table S6. Physicochemical properties and hydrophobic loading of hydrated nanocarriers after polymer-carbohydrate hydration.

Nanocarrier	Hydrophobic Cargo	Loading Efficiency (%)	Avg. Diameter (nm) <sup>†</sup>	PDI <sup>†</sup>	Zeta Potential (mV) <sup>††</sup>
C-MC	Curcumin	36.9 ± 2.5	24.3	0.08	-5.4 ± 0.8
C-PS	Curcumin	27.6 ± 1.6	68.9	0.30	-2.3 ± 0.4
Dex-TMR, Curcumin	Dex-TMR	16.3 ± 1.1	73.9	0.09	-1.8 ± 0.1
PS (dual loaded)	Curcumin	22.9 ± 0.4			

<sup>†</sup>Number-average diameter and polydispersity index (PDI) determined by dynamic light scattering (DLS).

<sup>††</sup>Zeta potential is reported as mean ± s.d.

**Table S7. Physicochemical properties of nanocarriers displaying cyclic RGD targeting peptides.**

Formulation	Avg. Diameter (nm) <sup>†</sup>	PDI <sup>†</sup>	Zeta Potential (mV) <sup>††</sup>
Dil MC	27.4	0.09	-1.1 ± 0.1
Dil MC +1% RGD	22.1	0.20	-1.3 ± 0.4
Dil MC +5% RGD	27.7	0.07	0.1 ± 0.9
Dex-TMR PS	111.8	0.16	-0.6 ± 0.2
Dex-TMR PS +1% RGD	87.5	0.14	-0.4 ± 0.2
Dex-TMR PS +5% RGD	84.2	0.17	4.1 ± 0.3

<sup>†</sup>Number-average diameter and polydispersity index (PDI) determined by dynamic light scattering (DLS).

<sup>††</sup>Zeta potential is reported as mean ± s.d.

**Table S8. Physicochemical characterization of hydrated nanocarriers self-assembled from powders containing commercially available polymers.**

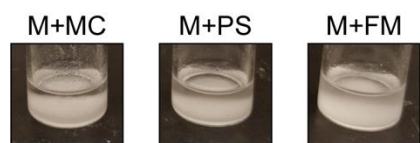
Nanocarrier	Loading Efficiency (%)	Avg. Diameter (nm) <sup>†</sup>	PDI <sup>†</sup>	Zeta Potential (mV) <sup>††</sup>
PEG- <i>b</i> -polystyrene	N/A	39.8	0.06	-8.5 ± 0.8
PEG- <i>b</i> -polycaprolactone	N/A	33.5	0.18	-3.2 ± 0.1

**Table S9. Commercial nanocarrier loading.**

Nanocarrier	Morphology	Cargo	Loading Efficiency (%)
PEG- <i>b</i> -polystyrene	Micelle	Dil (hydrophobic)	86.5 ± 4.4
PEG- <i>b</i> -polycaprolactone	Polymersome	Dil (hydrophobic)	45.5 ± 2.1
		Dex-TMR (hydrophilic)	9.6 ± 0.5

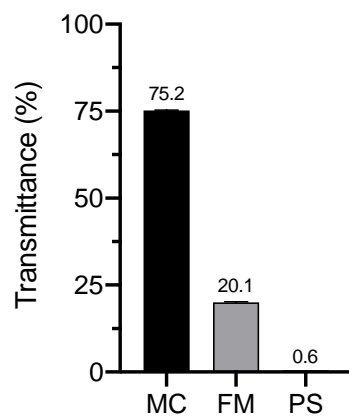
## Supplementary Media

**Supplementary Movie S1.** This video demonstrates the simplicity of hydration of nanocarrier-forming powders. The hydration of a powder consisting of PEG-*b*-PPS polymersome (PS) polymer and mannitol carbohydrate in a 1:3 polymer-to-carbohydrate ratio is presented as an example. The movie was acquired using a Celestron Handheld Digital Microscope Pro.

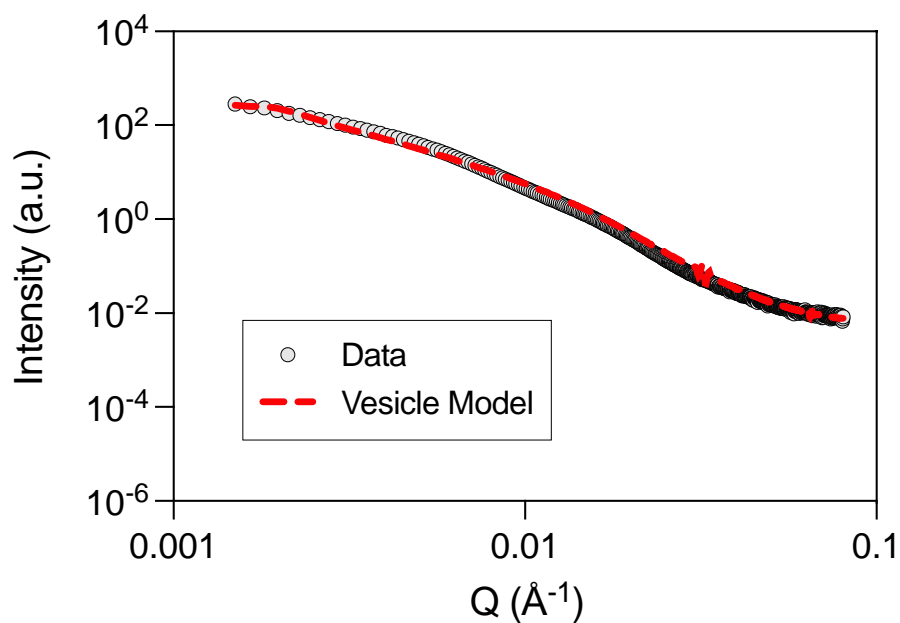
**Supplementary Figures**

**Fig. S1. Slurries of mannitol and PEG-*b*-PPS polymers in DCM prior to drying and powder formation.** A 3:1 ratio of carbohydrate:polymer was used to prepare each slurry.

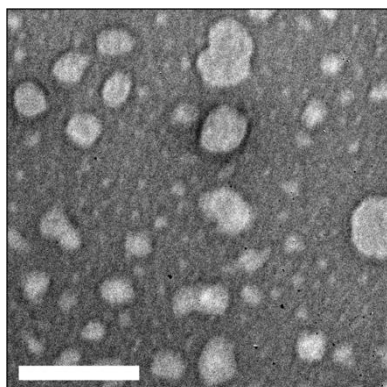




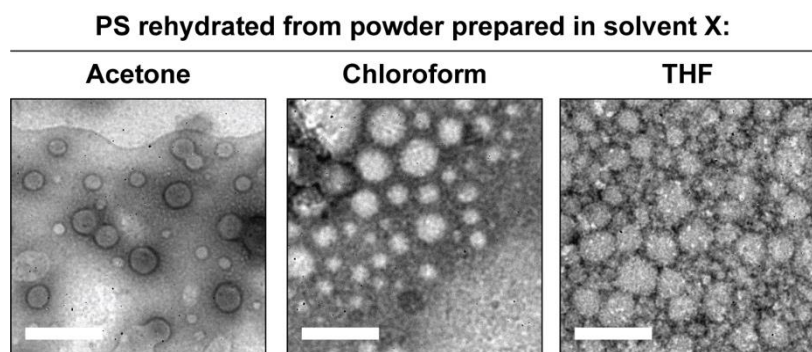
**Fig. S2. Percent transmittance of hydrated PEG-*b*-PPS nanocarrier formulations of diverse morphology.** The transmittance of 405 nm light was determined for hydrated micelles (MC), filomicelles (FM), and polymersomes (PS).



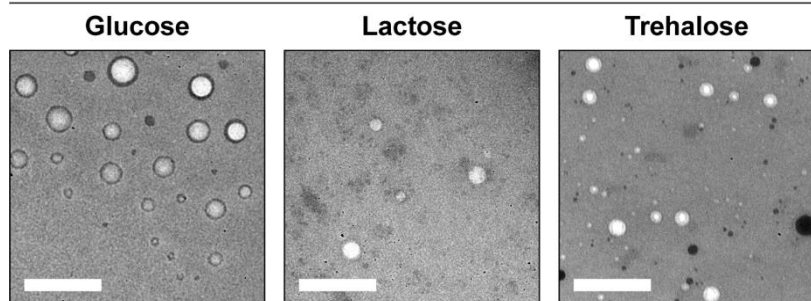
**Fig. S3. Small angle x-ray scattering (SAXS) of hydrated vesicular polymersomes.** SAXS was performed using synchrotron radiation at Argonne National Laboratory. A vesicle model was fit to the scattering profile of hydrated polymersomes (model fit:  $X^2 = 3.9$ ; radius = 47 nm; thickness = 7.8 nm).



**Fig S4. TEM micrograph of hydrated DiD-loaded PS suspension after 1 year storage at room temperature.** TEM micrograph was acquired at 30,000X. Scale bar = 200 nm.



**Fig. S5. PEG-*b*-PPS PS formed after hydration from polymer-carbohydrate powders formed in different solvents.** Powders were prepared by vacuum desiccation of acetone-, chloroform-, or THF-based slurries. TEM micrographs of the unpurified PS following hydration are displayed (30,000X; scale bar = 200 nm).

**PS rehydrated from powder containing carbohydrate X:**

**Fig. S6. PEG-*b*-PPS PS formed after hydration from polymer-carbohydrate powders formed using different carbohydrates.** Powders were prepared by vacuum desiccation of slurries composed of PEG-*b*-PPS PS polymer and the specified carbohydrate (glucose, lactose, or trehalose). TEM micrographs of the unpurified PS following hydration are displayed (30,000X; scale bar = 200 nm).

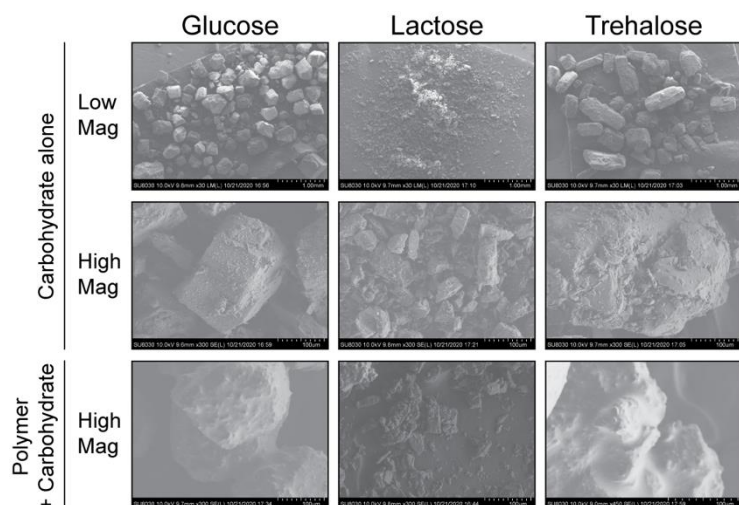


**Fig. S7. SEM micrographs of alternative carbohydrates and corresponding polymer-carbohydrate powders.** SEM micrographs at low magnification (top row) or high magnification (middle row) of free glucose, lactose, or trehalose carbohydrates are displayed. Micrographs of polymer-coated carbohydrates acquired at high magnification (300X or 450X) are displayed on the bottom row.

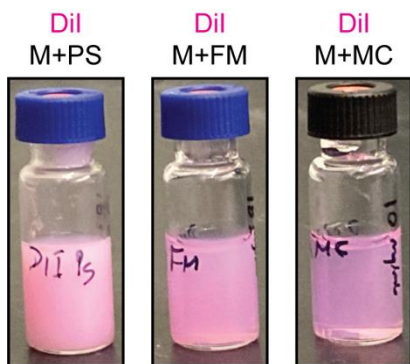


**Fig. S8. Images of Dil-loaded PEG-*b*-PPS nanocarriers of diverse morphology after hydration with PBS.** Dried powders consisting of mannitol carbohydrate, PEG-*b*-PPS polymer, and Dil drug were hydrated with PBS to a final polymer concentration of 10 mg/mL and were briefly vortexed to mix.

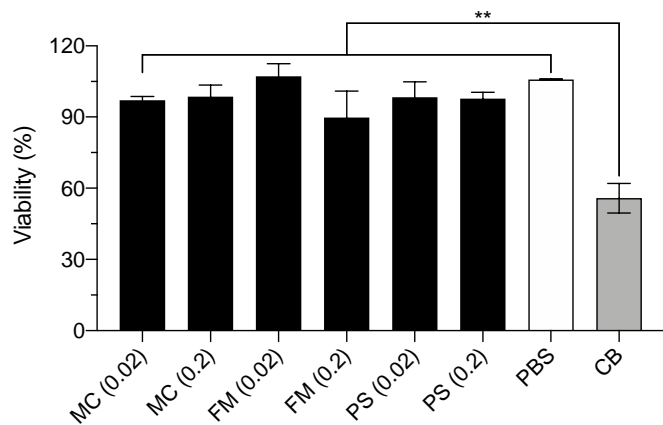


**Fig. S9. Assessment of cell viability using the MTT assay.** RAW 264.7 macrophages were incubated with hydrated nanocarriers at the indicated concentration (in mg/mL), or with mannitol (Mann; 3 mg/mL) or Carboplatin (CB; 1 mg/mL) for 24 h at 37 °C. The percentage of viable cells is displayed. Significant differences in cell viability versus the CB toxicity group was determined by ANOVA with Dunnett's multiple comparisons test and a 5% significance level. \*\* $p < 0.005$ .



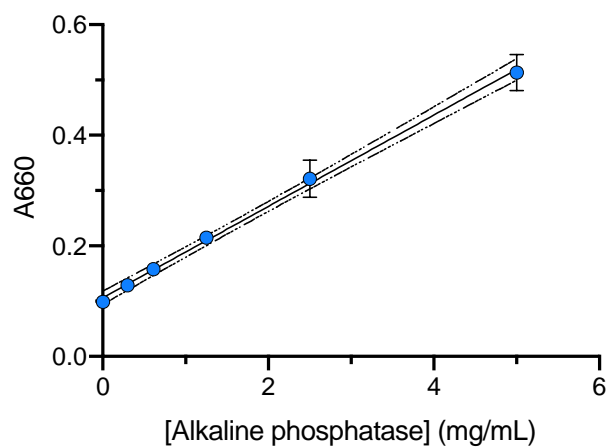


**Fig. S10. Calibration curve used to determine the concentration of loaded alkaline phosphatase enzyme.** The absorbance of 660 nm light of an alkaline phosphatase concentration series was measured in triplicate and the data were fit via a simple linear regression model ( $A_{660} = 0.08256c + 0.1063$ , where  $A_{660}$  is the absorbance of 660 nm light and  $c$  is the concentration (in mg/mL);  $r^2 = 0.9864$ ).

## References for Supporting Information

- 1 E. A. Scott, A. Stano, M. Gillard, A. C. Maio-Liu, M. A. Swartz and J. A. Hubbell, *Biomaterials*, 2012, **33**, 6211–6219.
- 2 S. Yi, S. D. Allen, Y.-G. Liu, B. Z. Ouyang, X. Li, P. Augsornworawat, E. B. Thorp and E. A. Scott, *ACS Nano*, 2016, **10**, 11290–11303.
- 3 N. B. Karabin, S. Allen, H.-K. Kwon, S. Bobbala, E. Firlar, T. Shokuhfar, K. R. Shull and E. A. Scott, *Nature Communications*, , DOI:10.1038/s41467-018-03001-9.
- 4 M. P. Vincent, S. Bobbala, N. B. Karabin, M. Frey, Y. Liu, J. O. Navidzadeh, T. Stack and E. A. Scott, *Nat Commun*, 2021, **12**, 648.
- 5 N. B. Karabin, M. P. Vincent, S. D. Allen, S. Bobbala, M. A. Frey, S. Yi, Y. Yang and E. A. Scott, *bioRxiv*, 2020, 2020.09.02.280404.
- 6 T. Stack, M. Vincent, A. Vahabikashi, G. Li, K. M. Perkumas, W. D. Stamer, M. Johnson and E. Scott, *Small*, 2020, 2004205.
- 7 M. P. Vincent, T. Stack, A. Vahabikashi, G. Li, K. M. Perkumas, R. Ren, H. Gong, W. D. Stamer, M. Johnson and E. A. Scott, *bioRxiv*, 2021, 2021.05.19.444878.
- 8 N. Nasongkla, X. Shuai, H. Ai, B. D. Weinberg, J. Pink, D. A. Boothman and J. Gao, *Angew Chem Int Ed Engl*, 2004, **43**, 6323–6327.
- 9 T. Mosmann, *J. Immunol. Methods*, 1983, **65**, 55–63.
- 10 Y. Wei, T. Tang and H.-B. Pang, *Nature Communications*, 2019, **10**, 3646.
- 11 L. Sasso, L. Purdie, A. Grabowska, A. T. Jones and C. Alexander, *Journal of Interdisciplinary Nanomedicine*, 2018, **3**, 67–81.
- 12 T. J. Chen and N. Kotecha, *Curr. Top. Microbiol. Immunol*, 2014, **377**, 127–157.